

Detonation Wave Velocity Error Calculation and Comparison of Methods

Regan Hencel, John Hoke
Innovative Scientific Solutions Inc.

Dayton OH, 45499
and

Matthew L. Fotia
Air Force Research Laboratory, Wright-Patterson AFB, 45433

1 Introduction

Experimental studies on RDE's often compare the experimental wave velocity to the 1-D theoretical Chapman-Jouguet velocity as an indication of operating mode as well as performance. Comparison of these two values is useful; however, this comparison fails to account for the differences between a measured velocity within an unsteady three-dimensional environment and the theoretical 1-D CJ velocity. Experimental studies have shown the measured detonation velocity can vary from 60% - 90% of the theoretical CJ velocity depending on the method used and the physical geometry of the test article. This has resulted in researchers utilizing additional tools to verify the presence of waves within a test article or calculating the speed of sound within the combustion chamber to verify that the measured detonation velocity is traveling supersonic. As the number of experimental investigations surrounding RDE's at both the industry and academic level continue to grow, little work has been done to quantify the error associated with the different types of measurement methods used to obtain an experimental detonation velocity. While the ability to quantify the error associated with each measurement method is important, especially when using this velocity within different performance metrics, understanding the differences in reported error as a function of the measurement method can help experimentalists determine which method will provide acceptable results. The focus of this work is to use a variety of measurement methods to experimentally quantify the detonation velocity and associated error.

2 Experimental Set Up

This work was completed using a 6-inch, optically accessible, air-breathing rotating detonation engine that utilized gaseous hydrogen as fuel. Air was supplied to the device axially, while fuel was introduced through jet-in-crossflow fuel injection from the inner diameter. Figure 1 depicts the experimental test article and identifies the critical instrumentation and design features for this work. An array of highspeed instrumentation was utilized during each test condition to obtain data that could be used to determine

Distribution Statement A: Approved for public release: distribution is unlimited (AFRL-2025-XXXX)

Correspondence to: regan.hencel.ctr@us.af.mil

the primary frequency present in the test article. Four highspeed PCB pressure transducers were circumferentially offset in the air manifold to capture pressure waves present due to combustion in the channel. Another four PCBs were axially offset in the combustion channel to investigate the changes in pressure signals as the channel length increased. All high-speed pressure transducers were sampled at a frequency of 1 MHz. The combustion chamber was manufactured so a sapphire window could be installed, allowing for a highspeed camera to capture the detonation wave as it propagates around the combustion channel. A Phantom TMX 7510 was placed perpendicular to the flow of combustion products and oriented such that the tangential propagation of these products could be viewed through the 2-inch x 3-inch sapphire window at a 265kHz capture rate.

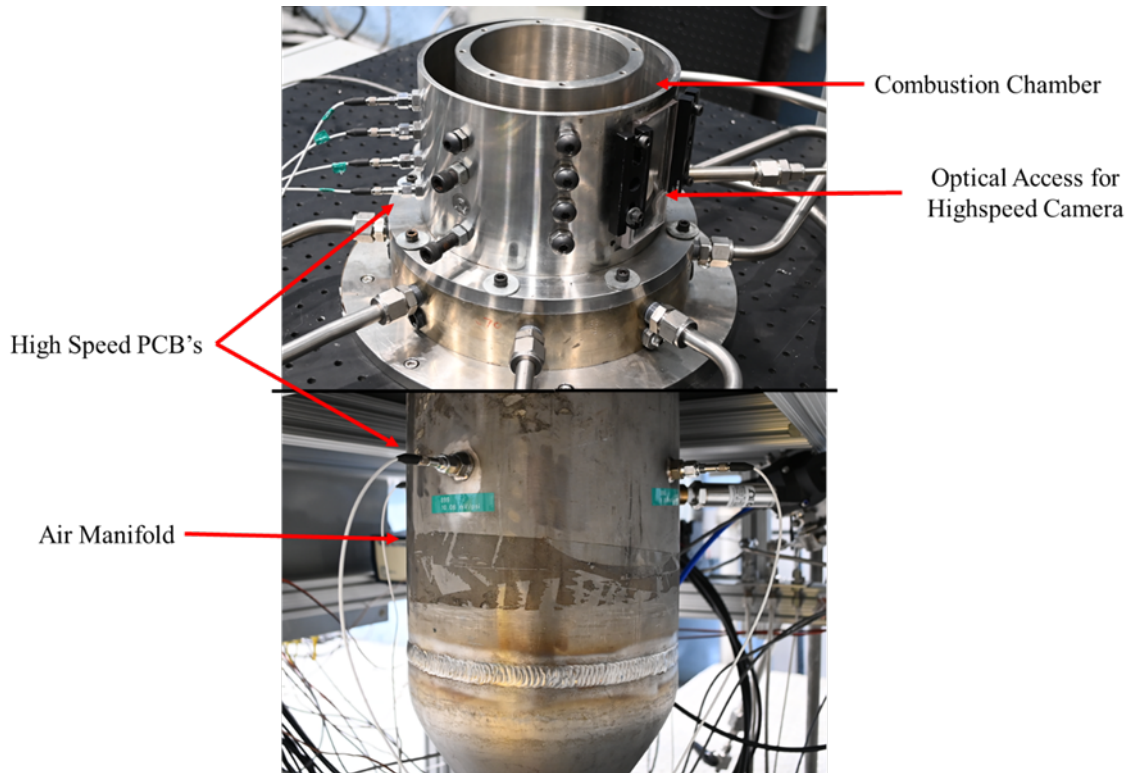


Figure 1: Experimental Test Article

3 Methods

The highspeed data collected during each test condition was used to calculate the resulting wave velocity and error. Each signal was clipped such that only the hot-fire portion of each test was analyzed and used to calculate these values three different ways. The first method was to feed each clipped data set directly into a Fast Fourier Transform to obtain the primary operating frequency, and ultimately the velocity, using Equation 1. The error associated with this method is correlated with the diameter of the PCB head itself as well as the sampling rate of the system, shown in Equation 2. In the following equations f represents frequency, C represents the circumference of the engine where the instrumentation is located, w_C represents the error on the circumference of the engine, which is the diameter of the PCB head, and w_f represents the error on the frequency based on the selected data and data sampling rate. It is important to note that the error on the frequency is influenced by data used to calculate the frequency as well as the sampling rate the data was collected at. Equation 3 shows the calculation for w_f , where Sample Number refers to the numerical order of the identified peak in the detrended dataset, and F_s refers to the sampling rate at which the data was collected.

$$V = f * C \quad \text{Equation 1}$$

$$w_v = \sqrt{(w_c^2 * f^2) + (w_f^2 * C^2)} \quad \text{Equation 2}$$

$$w_f = \frac{1}{\left(\frac{\text{Sample Number}_2 - \text{Sample Number}_1}{F_s}\right)} \quad \text{Equation 3}$$

The second and third methods require the clipped dataset to pass through a function that detrends the information by removing the best straight-fit line and returning what is left. This returned data is then passed through the MATLAB function “findpeaks” to determine the periodic local maxima and their location. Once the peaks have been identified, these methods use a selected region of the identified peaks to obtain the operating frequency. One way to determine the wave velocity using this information is to manually select two peaks in the dataset and calculate the frequency between these locations using Equation 4. The error associated with this method is calculated using Equation 5, where laps is the number of laps that occurred between the selected peaks in the dataset. The final method used to calculate the wave velocity was to use the same selected peaks discussed previously and calculate the change in wave position over time. Equations 6, 7, and 8 illustrate this calculation of the velocity and associated error, where runtime refers to the amount of time that has passed between the selected peaks in the detrended dataset and w_t is the error on the time reported by the DAQ system. For this work, w_t was a static value of $1 * 10^{-4}$.

$$f = \frac{1}{\text{Sample Number}_2 - \text{Sample Number}_1} * \frac{F_s}{\text{laps}} \quad \text{Equation 4}$$

$$w_v = \sqrt{(w_c^2 * f^2) + (w_f^2 * (\text{laps} * C^2))} \quad \text{Equation 5}$$

$$\text{runtime} = \frac{\text{Sample Number}_2 - \text{Sample Number}_1}{F_s} \quad \text{Equation 6}$$

$$V = \frac{\text{laps} * C}{\text{runtime}} \quad \text{Equation 7}$$

$$w_v = \sqrt{w_c^2 * \left(\frac{1}{\text{runtime}}\right)^2 + \left(w_t^2 * \left(\frac{\text{laps} * C}{\text{runtime}^2}\right)^2\right)} \quad \text{Equation 8}$$

To calculate the velocity using highspeed video, the video files were converted into image frames over the duration of the test condition, allowing them to be imported into MATLAB for image processing and analysis. Since the resolution for each image is known, each pixel has a corresponding intensity that can be averaged for every column of pixels. Three columns of pixels are then selected such that they are equidistant from one another, allowing the average intensity for each column to be plotted as a function of time. Velocity can be obtained by using a Fast Fourier Transform for a column of average intensities. This will provide a signal frequency that can then be used to calculate the velocity using Equation 1. The three columns of interest can also be used in a cross correlation, like the method previously discussed, to verify the primary operating frequency obtained by the FFT.

Figure 2 is a compilation of three frames of a highspeed chemiluminescence video from an optically accessible 6-inch RDE. In this figure the wave is propagating in a counterclockwise direction. The three red boxes on each image frame represent the columns of pixels used to obtain average intensity values over time. The average intensity of each column will vary over time as the wavefront

propagates around the combustion chamber, which can be fed into a FFT to obtain the frequency of the wavefront passing the same location. This same methodology was utilized for the chemiluminescence video capture through the sapphire window, discussed above.

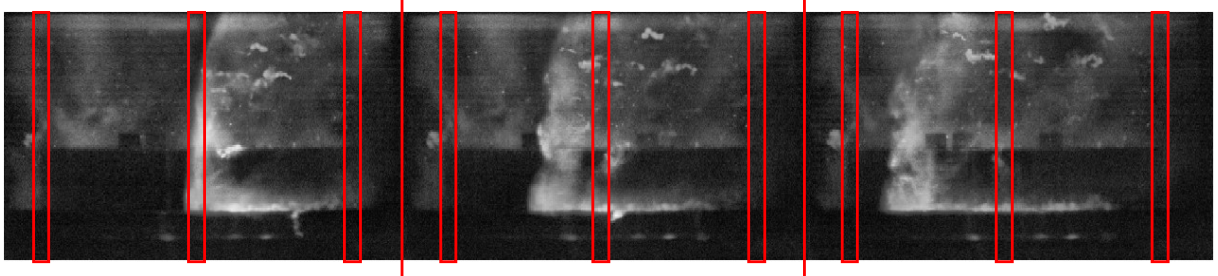


Figure 2: Highspeed Chemiluminescence Video – Frame Compilation

The peak identification techniques used in this work can produce varying results by adjusting the minimum peak prominence value. Figures 3 and 4 show the difference in the number of peaks identified using two different prominence values, 0.9 and 0.4 respectively. This highlights the importance of ensuring that a sufficient prominence value is selected. A sufficient prominence value was selected for this work by plotting the prominence value as a function of the average time between the identified peaks in a dataset, shown in Figure 5, which depicts an “S” curve. Selecting a prominence value that is in the plateaued region of this “S” curve ensures that the number of peaks identified by the algorithm are not influenced by the average time between the peaks. The following plots that use this peak identification method will have been done so using a prominence value of 0.9 unless otherwise stated.

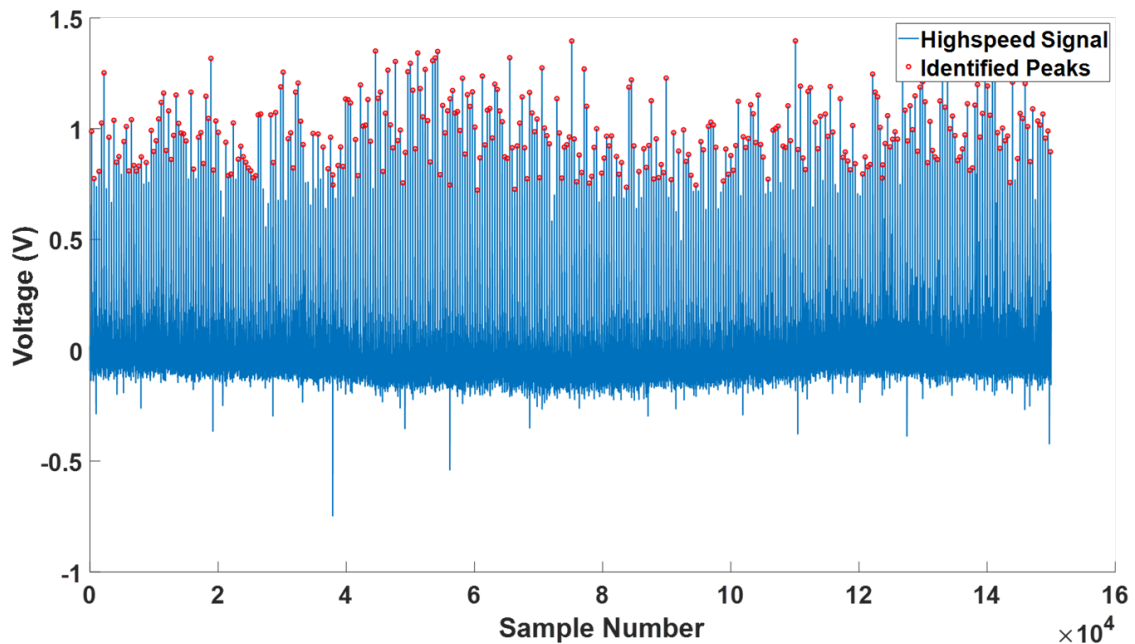


Figure 3: Minimum Peak Prominence = 0.9

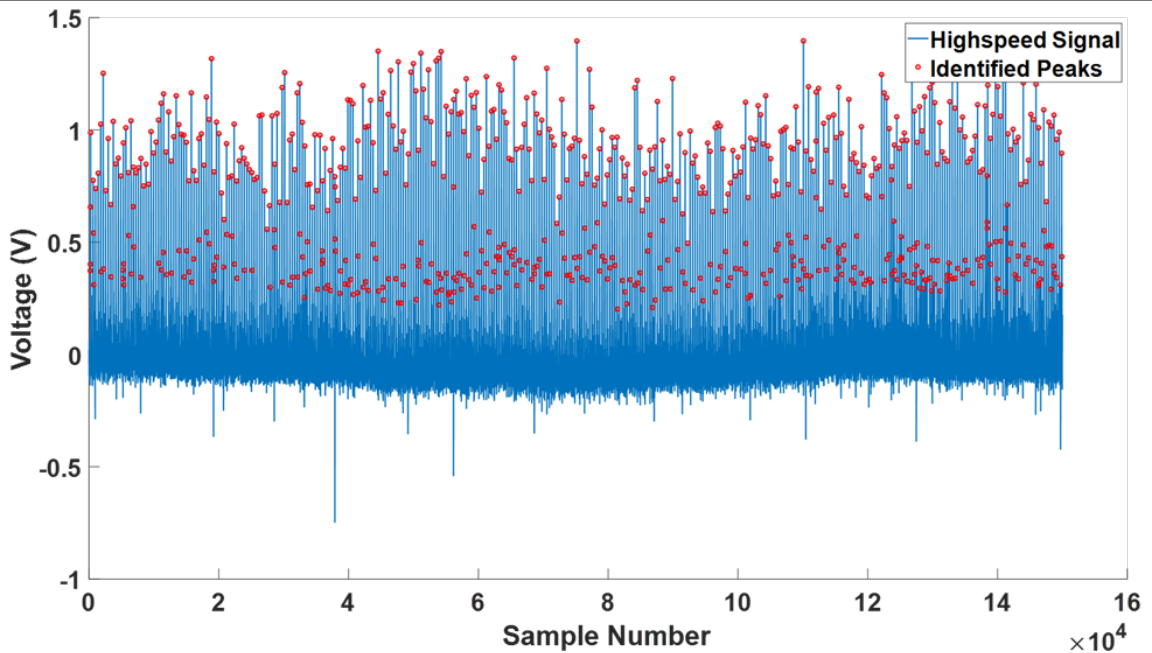


Figure 4: Minimum Peak Prominence = 0.4

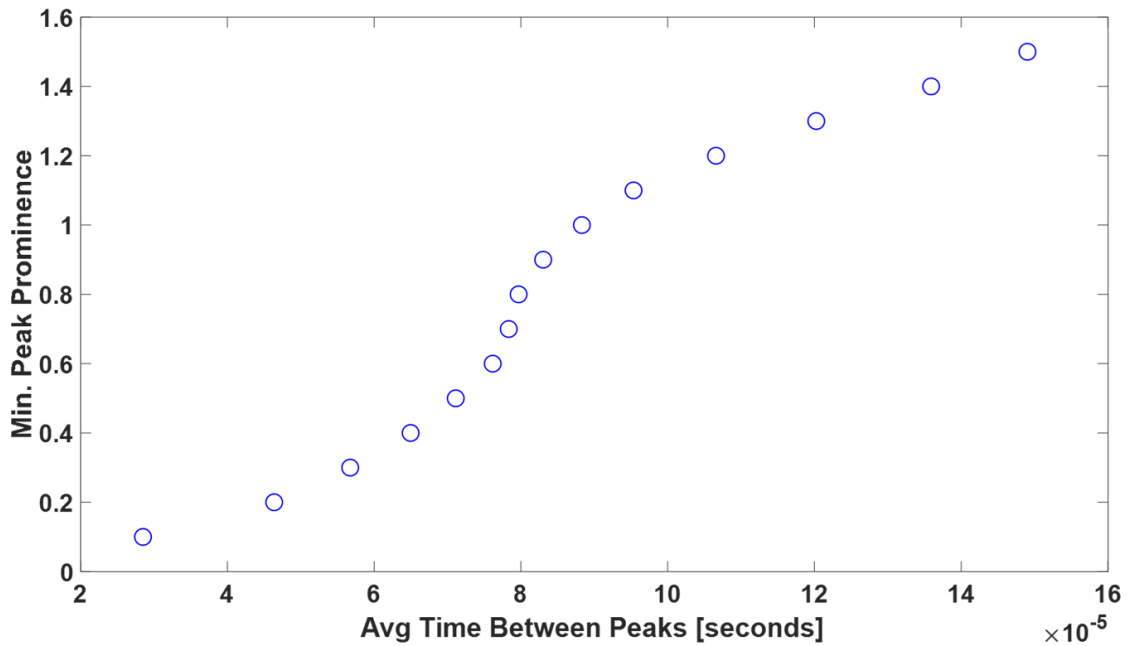


Figure 5: Minimum Peak Prominence as a Function of Average Time Between Peaks

4 Results

The goal of this work was to investigate the difference in calculated velocity and associated error using the methods describe above. Figure 6 depicts the calculated velocity and error for each method. This figure shows that each method produced a similar mean velocity, however the error produced by each method varies significantly. Feeding the clipped highspeed data set directly into an FFT produced the smallest error, typically less then +/- 5m/s. Using peak identification and manually selecting the region to analyze via a FFT to obtain the primary operating frequency produced error that was less than +/- 50m/s. The same manually selected region produced significantly more error, less than +/-100

m/s. It should be noted that the resulting error for methods 1 and 2 is dependent on how much of the original signal is being used to calculate the velocity. The data shown in Figure 6 was calculated using 5 sequential peaks located in the center of the dataset, a very small portion of the original signal. Using more of the original signal will result in lower errors on the calculated velocity. This is due to variations in the original signal being averaged out over time. Figure 7 plots a distribution of the lap-to-lap velocity across the entire signal using the identified peaks which shows a bimodal behavior that results in the mean velocity value having a larger spread.

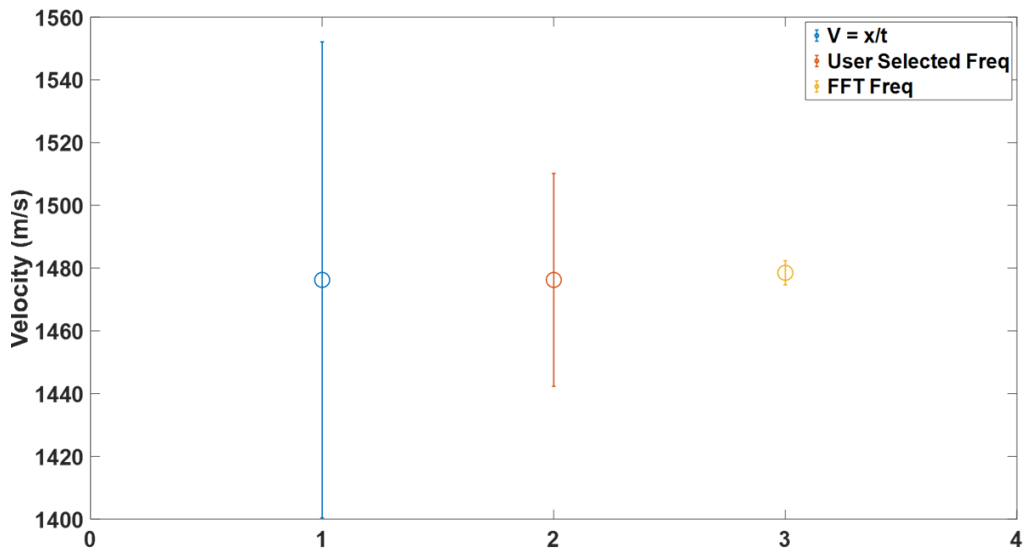


Figure 6: Velocity Calculation Method Comparison

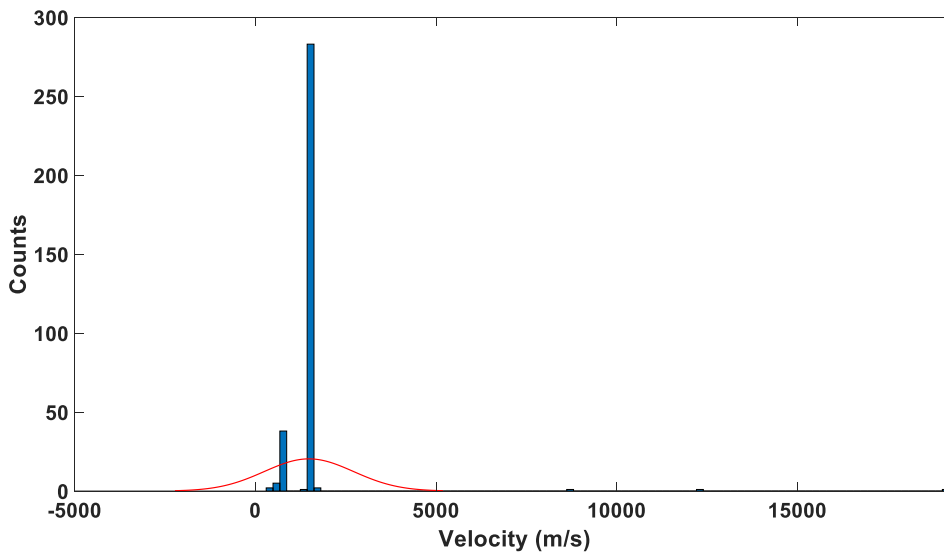


Figure 7: Lap-to-Lap Velocity Distribution of Identified Peaks

References

- [1] M. Stocke, R. Hencel, J. Hoke, M. L. Fotia, “Detonation Wave Velocity Error Across Multiple Methodologies in a 6-Inch Rotating Detonation Engine”, Presented at 63rd Aerospace Sciences Meeting, Orlando FL, AIAA 2025-1186, January 6-10, 2025